Geochimica et Cosmochimica Acta 424 (2026) 15–29

Contents lists available at ScienceDirect

Geochimica et Cosmochimica Acta

journal homepage: www.elsevier.com/locate/gca

Large seasonal and inter-annual variability in lipid biomarker fluxes: unique records of 4.5 years of monthly sediment-trap data from a tropical lake

J.S. Sinninghe Damsté [a,b,*], L.G.J. van Bree [a], J. Lattaud [b,1], P. de Regt [a], C. Cocquyt [c,d], A.J. Baxter [a], J.W. de Leeuw [a,b], D. Verschuren [c], F. Peterse [a]

[a] Utrecht University, Faculty of Geosciences, Department of Earth Sciences, Princetonlaan 8A, 3584 CB Utrecht, Netherlands (the)
[b] NIOZ Royal Netherlands Institute for Sea Research, Department of Marine Microbiology and Biogeochemistry, PO Box 59, 1790 AB Den Burg, Netherlands (the)
[c] Ghent University, Limnology Unit, K.L. Ledeganckstraat 35, B-9000 Ghent, Belgium
[d] Meise Botanic Garden, Research Department, Nieuwelaan 38, B-1860 Meise, Belgium

ARTICLE INFO

Associate editor: Meixun Zhao

Keywords:
Aquatic biomarkers
Organic geochemistry
Stable carbon isotopes
Sediment trap
Time series
Paleolimnology
Paleoclimatology

ABSTRACT

Lake Chala, a permanently stratified crater lake in tropical eastern Africa, provides a unique sedimentary record deposited continuously over the last 250,000 years. Biomarkers preserved in these sediments allow reconstruction of regional palaeoclimate history in unprecedented detail. However, for sound interpretation of the biomarker record a proper knowledge on their biological sources and factors influencing their production are a prerequisite. Previous studies on biomarkers derived from phytoplankton and vascular (terrestrial) plants in suspended particulate matter sampled monthly over almost 1.5 years revealed large seasonal variation in their distribution in the water column. Here we extend this time series to 4.5 years (September 2010 to January 2015) by analyzing biomarker fluxes in settling particles collected monthly by a sediment trap deployed at 35 m water depth. The flux of vascular plant lipids was overall low and irregular. Variation in phytoplankton biomarker fluxes indicate that aquatic microbial production and community composition in Lake Chala are strongly influenced by the seasonal succession of water-column stratification and deep but partial mixing. Fluxes of biomarkers representing Chlorophyte algae (long-chain *n*-alk-1-enes, C_{21} and C_{23} *n*-alkanes) and diatoms (loliolide and isololiolide) were highest during the deep mixing season, but not every deep mixing period elicited a strong phytoplankton response. Temporal variation in the flux of the *n*-C_{28} fatty acid, often used as a plant wax biomarker, resembles that of Chlorophyte biovolume and biomarkers, indicating an aquatic source with the Chlorophyte *Tetraedron minimum* as most likely producer. Large fluctuation in $\delta^{13}C$ values of the *n*-C_{28} fatty acid indicate regular occurrence of chemically enhanced fractionation at high pH. Fluxes of Eustigmatophyceae biomarkers (C_{30} and C_{32} long-chain diols) were highest during the period of stratification. Fluxes of the C_{19} *n*-alkene, which increase during periods of water-column stratification and/or shallow mixing, can be linked to cyanobacteria. Taking seasonal and interannual variability together, microbial production and productivity in the upper water column is primarily determined by the depth of seasonal water column mixing, as this controls the amount of nutrients being recycled from the hypolimnion. Large inter-annual variability of aquatic lipid biomarkers in the settling particles of Lake Chala indicates that small differences in ambient water-column conditions can cause strong turnover in the microbial communities, preventing systematic recurrence of a stable phytoplankton succession pattern. This implies that monitoring programs organized to capture the natural variability of lake systems must run for many years to fully reveal the relationship between biomarkers in the modern lake system and biomarker proxies in the sedimentary record used for paleoenvironmental reconstruction.

* Corresponding author at: Utrecht University, Faculty of Geosciences, Department of Earth Sciences, Princetonlaan 8A, 3584 CB Utrecht, Netherlands (the).
E-mail address: jaap.damste@nioz.nl (J.S. Sinninghe Damsté).
[1] Present address: Department of Environmental Science, Stockholm University, Stockholm, Sweden.

https://doi.org/10.1016/j.gca.2026.05.015
Received 21 December 2025; Accepted 12 May 2026
Available online 16 May 2026
0016-7037/© 2026 The Author(s). Published by Elsevier Ltd. This is an open access article under the CC BY license (http://creativecommons.org/licenses/by/4.0/).

1. Introduction

Sediments accumulating in lakes are natural archives of past environmental conditions which can be explored microscopically and chemically at high temporal resolution. At the molecular level, lipid biomarkers preserved in lake sediments are increasingly used to reconstruct past climate and ecosystem variability, based on the principle that these fossil lipids reflect the response of their producer(s) to (past) environmental changes (see Castañeda and Schouten, 2011 for a review). To properly link the presence and relative abundances of individual biomarkers with the environmental processes that drive their production or input over time, long-term monitoring of the modern lake system above these sediments is required. However, such extensive monitoring is not often implemented. Available studies either cover relatively short time intervals, i.e., up to one full year (e.g., Meyers et al., 1984; Russell and Rosell-Melé, 2005), and/or are limited to specific biomarker groups, such as long-chain diols (e.g., Villanueva et al., 2014; Lattaud et al., 2021), long-chain alkenones (e.g., Randlett et al., 2014; Longo et al., 2018), or bacterial and archaeal membrane lipids (Sinninghe Damsté et al., 2009, 2022; Woltering et al., 2012; Buckles et al., 2014, 2016; Loomis et al., 2014; van Bree et al., 2020; Baxter et al., 2021). Long-term (>1 year) lake monitoring studies that cover a wide array of biomarkers are scarce, especially in the tropics, which is problematic considering that these regions are underrepresented in the total volume of continental paleoclimate reconstructions.

One notable exception is Lake Chala, a deep and permanently stratified (meromictic) crater lake in eastern equatorial Africa. Long-term hydrological stability and permanently anoxic bottom water has promoted preservation of annually laminated sediments (varves), resulting in an impressive continuous sedimentary archive spanning the last 250,000 years (Moernaut et al., 2010; Martin-Jones et al., 2024). These conditions have also resulted in excellent long-term preservation of organic compounds. Lipid biomarkers in profundal Lake Chala sediments have been analyzed extensively to reconstruct past changes in regional temperature and moisture balance (Verschuren et al., 2009; Tierney et al., 2011; Sinninghe Damsté et al., 2011; Buckles et al., 2016; Baxter et al., 2023), regional vegetation (Sinninghe Damsté et al., 2011; van Bree et al., 2016), lake-basin evolution (Baxter et al., 2024) and phytoplankton productivity (van Bree et al., 2014, 2018a). Among several previous studies focusing on the distribution and possible sources of lipid biomarkers in modern-day Lake Chala (e.g., Buckles et al., 2013, 2014; Baxter et al., 2021), van Bree et al. (2018b) aimed to investigate a wide array of biomarker-based paleo-environmental proxies by assessing their occurrence in suspended particulate matter (SPM) collected over 17 consecutive months (September 2013 to January 2015) at 13 discrete depths in the 90 m deep water column. This comprehensive analysis revealed unexpected sources and processes driving the local presence of several lipid biomarkers. Firstly, terrestrial biomarkers were nearly absent in SPM throughout the studied interval, even though plant leaf-wax biomarkers such as long-chain *n*-alkanes and des-A-lupane are clearly present in the sediment record (Sinninghe Damsté et al., 2011; van Bree et al., 2016). Secondly, the *n*-C_{28} fatty acid (FA), normally considered to be derived from leaf waxes of terrestrial vascular ('higher') plants, appeared to have a primary aquatic origin (van Bree et al., 2018b). This is noteworthy since this FA is generally abundant in tropical African lake sediments, and its stable isotopic composition is often used in paleovegetation ($\delta^{13}C$) or paleohydrological ($\delta^{2}H$) reconstructions (e.g., Eglinton and Eglinton, 2008; Tierney et al., 2008; Castañeda and Schouten, 2011; Berke et al., 2012; Freeman and Pancost, 2014; Hemingway et al., 2016). The apparent aquatic rather than vascular plant source of this FA has important implications for the paleoenvironmental interpretation of these records. Thirdly, a special process of stable carbon-isotope fractionation was found to occur during seasonal episodes with elevated epilimnetic pH (>8) and high production of aquatic biomarkers. Chemically enhanced diffusion of atmospheric CO_2 into the lake resulted in unusually strong fractionation of the carbon isotopes, and hence exceptionally depleted $\delta^{13}C$ signatures of aquatic biomarkers (van Bree et al., 2018b). Understanding the occurrence and extent of this process over longer time scales is imperative as it may affect the $\delta^{13}C$ values of aquatic biomarkers and, consequently, also that of the bulk organic matter stored in the lake sediments.

Given the potentially large impact of the above-mentioned processes on the interpretation of sedimentary biomarker records, it is important to assess whether the seasonal trends in biomarker distribution revealed by the 17-month SPM study are annually recurrent on longer time scales. Two previous studies of glycerol dialkyl glycerol tetraethers (GDGTs) in the modern system of Lake Chala compared trends in the 17-month SPM record to monthly variations in settling particles collected over 4.5 consecutive years by a sediment trap at 35 m water depth, and concluded that environmental conditions during the 17-month period of SPM collection were atypical, resulting in biomarker distributions not fully representative of average modern-day ecosystem dynamics (van Bree et al., 2020; Baxter et al., 2021). To determine the extent to which this phenomenon affects other biomarkers, we now studied the temporal distribution of a wider array of lipid biomarkers in sediment-trap particles collected over the same 4.5-year period (September 2010 to January 2015). Overlap with the period of SPM-based data (van Bree et al., 2018b) enables us to assess for the first time both intra- and interannual variation in biomarker distributions in a tropical lake. Furthermore, to evaluate possible sources we compare biomarker fluxes to phytoplankton biovolume estimates obtained from the same material. Settling particles are an important link between the input or local production of biomarkers and those preserved in the sediment record. Hence, this study may reveal crucial information on the environmental parameters that drive the temporal dynamics of biomarker production and sources in lakes, and thus help constrain the paleoenvironmental significance of their occurrence and composition in lacustrine sediments.

2. Material and methods

2.1. Study site

Lake Chala (locally "Challa", after a nearby village) is a ~90 m deep crater lake bridging the border of Kenya and Tanzania in the foothills of Mt. Kilimanjaro (3°19'S, 37°42'E; Fig. 1A), just south of the equator in eastern tropical Africa. The lake is situated at ~880 m above sea level and has a surface area of 4.2 km^2. As lake-surface evaporation (~1700 mm yr^{-1}; Payne, 1970) exceeds local precipitation (~600 mm yr^{-1}, with large interannual variability), the lake is maintained at its present surface level by subsurface groundwater input, most likely originating from the forest belt and adjacent subalpine zone on Mt. Kilimanjaro (Hemp, 2006; Bodé et al., 2020). The rain belt trailing the Inter-Tropical Convergence Zone (ITCZ) passes over Lake Chala twice yearly, resulting in two distinct rain seasons, with relatively heavy 'short rains' from October to December and 'long rains' from March to May (Nicholson, 2000; Verschuren et al., 2009). Wind-driven and night-time convective mixing produces a principal thermocline fluctuating between 10 and 20 m depth through the year. High temperature and slack winds during the rainy seasons lead to strongly stratified water-column conditions, while higher windiness in January-February and especially during the cooler southern hemisphere winter (June-September) erode the thermocline and promote water-column mixing to greater depth, although the lake never turns over completely. Mostly depending on air temperature minima during this main dry season, deep mixing (DM) extends down to ~45–50 m, while shallower mixing (SM) to 25–30 m occurs during the short dry season (Buckles et al., 2014; van Bree et al., 2018b). The lower water column of Lake Chala displays density stratification preventing mixing deeper than ~55–60 m, and consequently profundal and bottom waters are permanently stratified and anoxic (Buckles et al., 2014; Baxter et al., 2024). Convective upwelling during deep mixing recycles

nutrients back into the photic zone, initiating a seasonal phytoplankton bloom dominated by diatoms. As variation in both air temperature and winds is important for the seasonal cycle of stratification and mixing in equatorial lakes (De Crop and Verschuren, 2021), the exact timing and duration of SM and DM periods in Lake Chala varies between successive years under the influence of multi-annual weather patterns such as the El Niño Southern Oscillation (ENSO) (Wolff et al., 2011; van Bree et al., 2020).

2.2. Sample collection

The sediment-trap deployment and sample collection has been described previously (e.g., Sinninghe Damsté et al., 2009; Buckles et al., 2014, 2016; van Bree et al., 2020). In short, a double-funneled sediment trap (UWITEC, 86 mm diameter) was installed in November 2006 at 35 m water depth in a mid-lake position (Fig. 1B), and emptied and redeployed at monthly intervals. This study focuses on the 53 monthly samples collected between September 2010 and January 2015. Collected material was allowed to settle for two days before excess water was decanted and the remaining material was stored frozen. The sediment-trap samples were thawed to allow sub-sampling for quantitative analysis of phytoplankton remains. These sub-samples were kept in a fridge until microscopic analysis. The remaining material was filtered over pre-weighed and pre-combusted (400 °C, 5 h) glass fiber GF/F filters (110 mm diameter, Whatmann) and stored frozen until further analysis.

2.3. Sample preparation, extraction and instrumental analysis of lipid biomarkers

Lipid extraction from the sediment-trap material has been described in detail by van Bree et al. (2020) and Baxter et al. (2021). In short, the filters with sediment-trap material were freeze-dried, cut into small pieces and directly acid hydrolyzed with 1.5 N hydrochloric acid (HCl) in methanol (MeOH) with a known stable carbon isotopic composition. After 2 h reflux at 80 °C, the pH was adjusted to 4–5 with potassium hydroxide (KOH) / MeOH, prior to liquid–liquid extraction (three times) with dichloromethane (DCM). The combined supernatant was dried under N_2, water was removed with a Na_2SO_4 column, and again dried under a stream of N_2. This total lipid extract was separated on an activated Al_2O_3 column into an apolar, neutral and polar fraction, using hexane/DCM (9:1, v/v), DCM, and DCM/MeOH (2:1, v/v) as eluents, respectively. A known amount of pristane (apolar fractions) or 5α-cholestane (other fractions) was added as internal standard.

The lipid biomarkers in all fractions were analyzed on a Hewlett Packard 6890 gas chromatograph (GC) equipped with a flame ionization detector (GC-FID). All fatty acids were measured as their methyl-ester derivatives, and polar fractions were silylated using N,O-bis-trimethylsilyl-trifluoroacetamide (BSTFA) and pyridine. The biomarker fractions (dissolved in hexane or ethyl acetate) were injected on-column at 70 °C, with helium as carrier gas with a flow rate of 2 ml min^{-1}. The oven was programmed to 130 °C at 20 °C min^{-1}, and then at 4 °C min^{-1} to 320 °C, and held isothermal for 10 min. Selected samples were analyzed for biomarker identification on a GC–mass spectrometer (GC–MS; Finnigan Trace GC Ultra, DSQ MS) with similar column properties and temperature program as applied for the GC analysis. The mass spectral identification of biomarkers was based on retention times, comparison with a NIST library and interpretation of mass spectral fragmentation patterns. Biomarkers were quantified based on comparison of their peak areas in the GC-FID chromatograms with that of the internal standard used. Biomarker fluxes were calculated from the amount of biomarkers in the monthly collected particulate matter in the sediment trap, the number of days of collection, and the surface area of the sediment trap (58 cm^2), and expressed in μg m^{-2} d^{-1}.

The carbon preference index (CPI) and average chain length (ACL) of the *n*-alkanes were calculated as:

$$CPI = 0.5*[\{\Sigma C25 - C33(odd)\}/\{\Sigma C26 - C34\ (even)\}] + 0.5*[\{\Sigma C25 - C33\ (odd)\}/\{\Sigma C24 - C32\ (even)\}] \quad (1)$$

$$ACL = \Sigma(Cn*n)/\Sigma Cn \quad (2)$$

where Cn is the abundance of each *n*-alkane with n carbon atoms. For the calculation of the ACL n ranges from 23–35.

For the detection and quantification of the long-chain diols (LCDs), aliquots of silylated polar fractions were analyzed as described in Lattaud et al. (2018). Briefly, LCDs were identified and quantified via Single Ion Monitoring (SIM) of the ions at *m/z* 299.3 (C_{28} 1,14-diol, C_{30} 1,16-diol), 313.3 (C_{28} 1,13-diol, C_{30} 1,15-diol), 327.3 (C_{30} 1,14-diol), 339.3 ($C_{32:1}$ 1,15-diol) and 341.3 (C_{30} 1,13-diol, C_{32} 1,15-diol, C_{34} 1,17-diol) (Rampen et al., 2012; Versteegh et al., 1997). Absolute concentrations

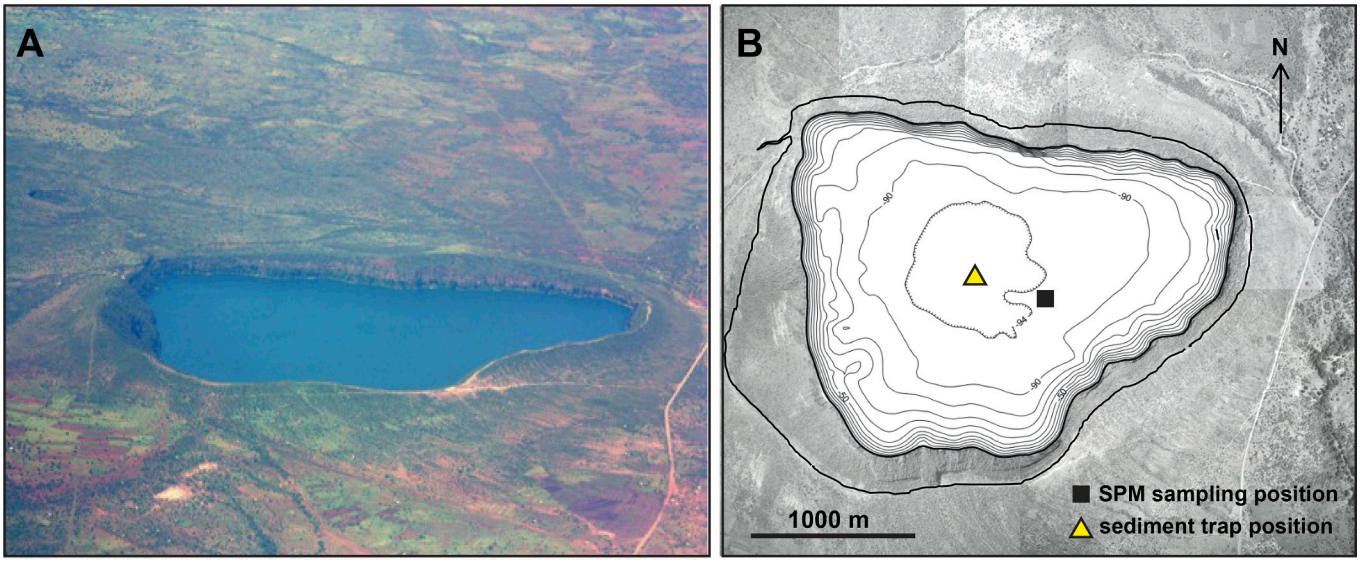


Fig. 1. Lake Chala (Kenya/Tanzania; 3°1ṕ S, 37°4ź E) and its crater catchment. (A) Oblique aerial view of the lake within its steep-sided crater basin, seen from the south. (B) Aerial-photograph mosaic of the crater area with outer full line indicating the crater rim, bathymetry with isopleths at 10-m intervals (adapted from Moernaut et al., 2010), and sampling positions of settling particles (sediment trap at 35 m depth; triangle) and SPM (van Bree et al., 2018b).

were calculated using the C_{22} 7,16-diol as internal standard, which was quantified with a SIM of the ion at *m/z* 187.2. Samples from September 2010 to July 2011 were no longer available for LCD analysis.

Samples selected for compound-specific $\delta^{13}C$ analysis were measured with GC combustion isotope-ratio-monitoring MS (GC-C-irmMS) an a ThermoFinnigan Delta Plus XP instrument using similar column properties and temperature program as applied for GC-FID analyses. GC-C-irmMS performance was checked daily by injection of a Schimmelmann alkane standard. The $\delta^{13}C$ values are expressed in ‰ versus the VPDB standard. Fatty acid $\delta^{13}C$ values were corrected for the methyl carbon atom added during acid methanolysis. The reported values are based on at least duplicate analyses, with results averaged to obtain a mean value and standard deviation. The standard deviations obtained were <0.7‰ for fatty acids and *n*-alk-1-enes, and <0.2‰ for *n*-alkanes.

2.4. Phytoplankton abundance

Phytoplankton biovolume flux estimates from the sediment-trap material were determined as reported in van Bree et al. (2018b). In short, the major groups of pelagic phytoplankton (Chlorophytes, diatoms, Dinophytes, Euglenophytes, Chrysophytes, Cryptophytes and cyanobacteria) were identified and counted with an inverted Olympus CKX41 microscope equipped with an Olympus UC30 digital camera, following the Utermöhl method (Utermöhl 1931, 1958) using sedimentation chambers of 10 ml. At least 500 solitary phytoplankton cells (≥3 μm) or colonies were counted per sample, as well as the number of cells per colony. The total biovolume of each taxon was calculated using known mean cell dimensions of represented species, and its flux was expressed in $\mu m^3\ m^{-2}\ d^{-1}$. Due to the minimum cell size of microscopy-based biovolume estimates, a significant component of photosynthetic picoplankton (<3 μm; mainly cyanobacteria and Chlorophytes) may not have been taken into account, but counts did include colonies of small coccoid cyanobacteria such as *Aphanothece* and *Aphanocapsa*.

3. Results and discussion

To link biomarker distributions with environmental processes, we studied biomarker fluxes in settling particles collected monthly at 35 m water depth with a sediment-trap in Lake Chala over 4.5 annual cycles of stratification and mixing with a monthly resolution.

3.1. Biomarkers for aquatic primary production

Monthly fluxes of biomarkers derived from aquatic primary producers are compared with biovolume data of the principal phytoplankton taxa. We then compared these biomarker and phytoplankton flux patterns with their abundances as measured in SPM depth profiles during a shorter, but overlapping time period (just over one annual cycle; van Bree et al., 2018b). An important caveat to this comparison is that settling particles and SPM reflect different aspects of biomarker production and transport to the sediment. Namely, as the sediment trap captures settling particles continuously, the biomass and lipid biomarkers captured reflect the average flux at 35 m water depth over the course of approximately one month. On the other hand, biomarker abundance in SPM represents a ‘snapshot’ situation reflecting only that particular time of sampling (van Bree et al., 2018b) and more likely contains living and, to some extent, decaying organisms.

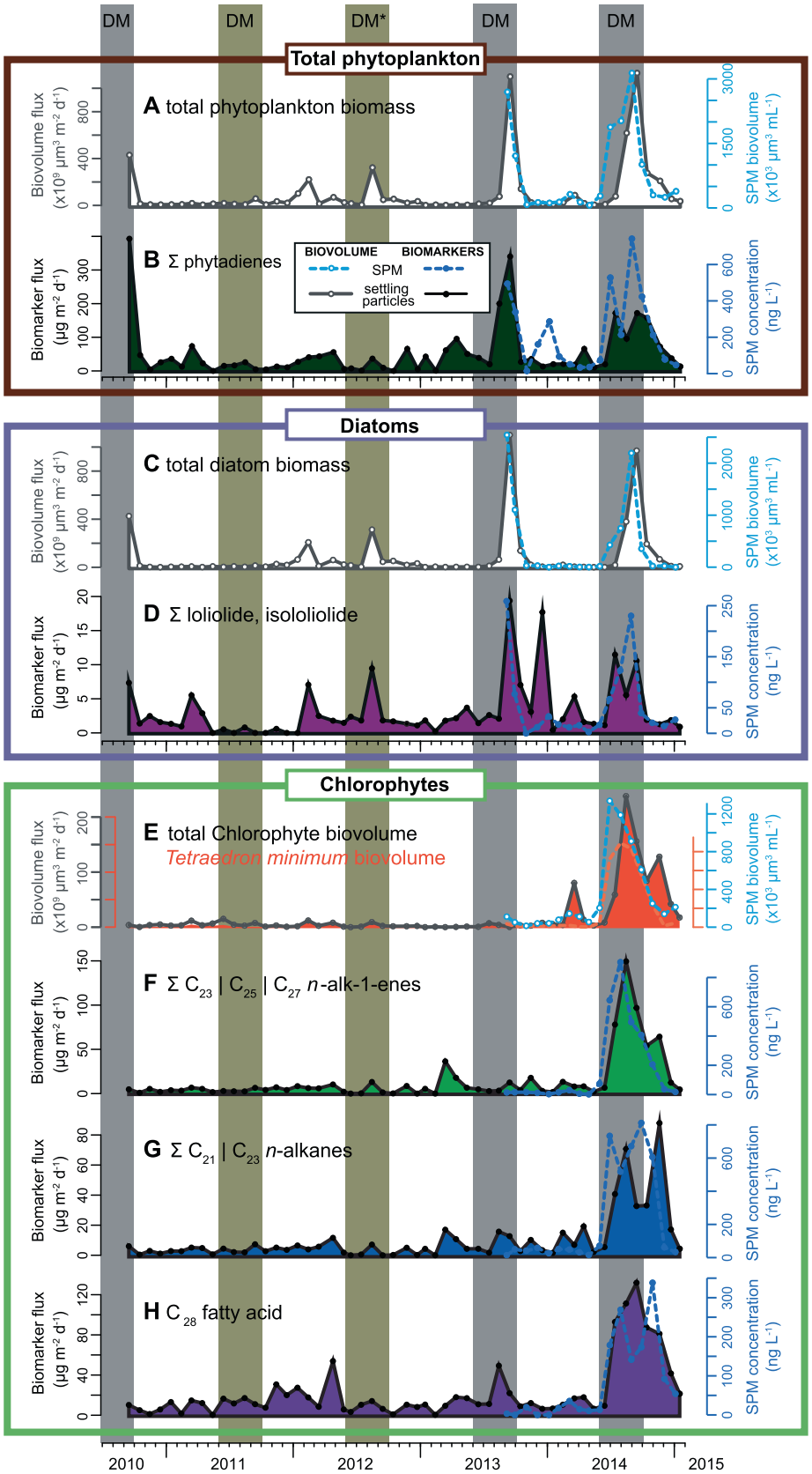
The total biovolume of phytoplankton in settling particles displays large seasonal and inter-annual variation; it is usually highest at the end of the DM season and the start of the subsequent stratification season, especially in September 2010, 2013 and 2014 (Fig. 2A). This is consistent with the fact that DM recycles nutrients from the hypolimnion to the photic zone, stimulating primary production. The higher total biovolume of phytoplankton in 2013–2014 than in 2011–2012 likely resulted from the greater depth of DM in 2013 as revealed by temperature-logger data (Buckles et al., 2014; van Bree et al., 2018b, 2020). Unusually cool weather in June-July 2013 forced a 0.2 °C decrease of water temperature at 50 m (from 22.5 °C to 22.3 °C), testifying to mixing deep enough to erode the top of the chemocline and hence providing unusual access to the massive but normally “locked” deep-water nutrient reservoir in the permanently stratified lower water column. Buckles et al. (2013) and Wolff et al. (2014) have documented earlier occurrences of this process in water column profiles of ammonium, nitrate, and soluble reactive phosphorous. Persisting into the next year, this slight but crucial temperature decline to 50 m depth also supported the strong phytoplankton bloom during DM in 2014. In contrast, in 2011–2012, DM only recycled nutrients released by decaying phytoplankton from the previous mixing/stratification cycle, which had accumulated in the hypolimnion not yet sunk into the deepwater zone below 50 m. This explanation rests on nutrient data from stratified, SM and DM periods collected between 2006 and 2010 (Buckles et al. 2013; Wolff et al. 2014). However, in this tropical meromictic lake we can expect that very similar nutrient profiles prevailed in these respective seasons during the 4.5-year period of sediment trap deployment.

The 17-month (September 2013 to January 2015) time series of total phytoplankton biovolume generated by analysis of live phytoplankton in the SPM from 0-20 m depth (stippled line in Fig. 2A; van Bree et al., 2018b) is fairly similar to that recorded by settling particles during the same period (full line in Fig. 2A; this study), suggesting that monthly variation in the flux of total biovolume settling at 35 m depth is indeed a good reflection of variation in the primary productivity of Lake Chala. The small discrepancies in biovolume estimates of SPM and sediment trap material may be caused by a component of decaying phytoplankton in the trap material that could not be identified to taxon level.

In our SPM study (van Bree et al., 2018b), we noted the presence of phytadienes, which following Grossi et al. (1996) were interpreted to be transformation products of chlorophyll-derived phytol produced by acid hydrolysis of the extract. The 17-month time series of their concentration in SPM integrated over the 0–25 m depth interval is similar to that of total phytoplankton biovolume (stippled lines in Figs. 2A-B), which is to be expected if the principal source of the trapped chlorophyll is aquatic phytoplankton. Similarly, phytadiene flux in the 53-month settling particle record correlates (R^2 = 0.55) with total phytoplankton biovolume flux (Figs. 2A-B). Background fluxes at times of low primary production are higher for phytadiene than for total biovolume but this is probably due to the presence of chlorophyll in (partly) degraded phytoplankton cells. Therefore, the flux of phytadienes recorded in settling particles may be a useful proxy for primary productivity.

3.1.1. Diatom biomarkers

Diatoms, especially the species *Afrocymbella barkeri* and *Nitzschia fabiennejansseniana* (Cocquyt and Ryken, 2016, 2017), are the dominant primary producers in modern-day Lake Chala. This is caused by (i) the all-year high Si concentration in the lake caused by the presence of easily weathered volcanic rocks (Wolff et al., 2014), and (ii) in contrast to smaller African crater lakes (e.g., Nankabirwa et al., 2019) Lake Chala is large enough to create a turbulent upper water column keeping diatoms afloat at least during the windy DM season. Diatoms are also abundant throughout the sedimentary record, suggesting they have always been major contributors to primary production in this lake (e.g., Barker et al., 2011; Wolff et al., 2014). In our settling particle data they constitute between 5.8 and 100% (63 ± 30% on average, n = 53) of total biovolume over the period of sediment-trap deployment. The time series of diatom biovolume flux is highly similar to that of the total biovolume flux (Fig. 2C and A; R^2 = 0.97) because at the times of maximum biovolume flux, diatoms comprise its largest fraction (>90%). Monthly diatom biovolume flux in the settling particles closely traces that of diatom biovolume in SPM, indicating that with respect to diatom production, the diatom biovolume flux at 35 m is a good reflection of what is happening in the surface waters of the lake.



(caption on next page)

Fig. 2. Biovolume and biomarker fluxes of total and specific phytoplankton, and of diatom and Chlorophyte biomarkers in Lake Chala, respectively, at monthly intervals between September 2010 and January 2015 determined from settling particles at 35 m water depth. For comparison, average phytoplankton biovolume (0–10-20 m) and average biomarker concentration in surface-water SPM (0–10-25 m) between September 2013 and January 2015 (van Bree et al., 2018b) are shown. Data for settling particles are plotted on the median day of the monthly sediment-trapping interval; SPM data are plotted on the day of sampling. The vertical bands indicate the annual period of deep mixing (DM; June – September) as determined by automated temperature logging (Buckles et al. 2014) or monthly profiling (van Bree et al. 2018b, 2020). The depth and duration of DM varied between years; grey bands indicate deeper mixing than those coloured olive green. The asterisk (*) indicates that the end of the 2012 DM period is uncertain due to logger malfunctioning. (A) Total phytoplankton biovolume flux in settling particles (solid gray line) and SPM biovolume of total phytoplankton in surface waters (dashed light blue line; this excludes heterotrophic dinoflagellates). (B) Flux of phytadienes in settling particles (solid black line) and their concentration in surface-water SPM (dashed blue line). (C) Total diatom biovolume flux in settling particles (solid gray line) and SPM biovolume in surface waters (dashed light blue line). (D) Summed flux of (iso)loliolide in settling particles (solid black line) and their summed concentration in surface-water SPM (dashed blue line). (E) Total Chlorophyte biovolume flux in settling particles (solid black line), and specifically for *Tetraedron minimum* (solid orange line), and SPM biovolume of Chlorophytes (and *T. minimum*) in surface waters (dashed blue and orange line, respectively). (F) Summed flux of C_{23}, C_{25} and C_{27} *n*-alk-1-enes in settling particles (solid black line) and their concentration in surface water SPM (dashed blue line). (G) Summed flux of C_{21} and C_{23} *n*-alkanes in settling particles (solid black line) and their summed concentration in surface-water SPM (dashed blue line). (H) C_{28} fatty acid flux in settling particles (solid black line) and its concentration in surface-water SPM (dashed blue line).

Loliolide and isololiolide are relatively stable degradation products of the diatom pigment fucoxanthin (Klok et al., 1984; Repeta, 1989) and, therefore, often used as biomarkers for diatoms (e.g., Castañeda and Schouten, 2011; van Bree et al., 2018b), although some haptophyte and dinophyte species have also been reported to contain fucoxanthin (Klok et al., 1984; Jeffrey and Vesk, 1997). High (iso)loliolide fluxes at 35 m correspond reasonably well ($R^2 = 0.52$) with peaks in diatom biomass (Figs. 2C-D). In a few monthly intervals (iso)loliolide fluxes were high when diatom biovolume was low (March to April 2011, December 2013, and March 2014; Figs. 2C-D), potentially indicating a secondary, non-diatom source of (iso)loliolide. For example, a Dinophyte bloom in March and April 2014 (van Bree et al., 2018b) may be responsible for the small peak in the (iso)loliolide flux in March 2014.

Generally speaking, highest diatom production occurred during the DM periods, when upcycled nutrients are able to sustain diatom blooms (Figs. 2C-D). However, the peak values of diatom biovolume and biomarker fluxes, and to a lesser extent the inferred duration of diatom blooms vary substantially between successive DM periods; diatom blooms do not even systematically recur every year. The highly variable flux between October 2010 and July 2013 with modest diatom blooms across two annual cycles of mixing and stratification, suggests that nutrient availability in the photic zone varies between successive years, likely due to subtle differences in environmental conditions such as the depth of DM, as discussed for the total phytoplankton biovolume. We note that diatom fluxes were overall highest during the period of SPM sampling (September 2013 to January 2015).

3.1.2. Chlorophyte biomarkers

After diatoms, Chlorophytes (green algae) are the most important phytoplankton group in Lake Chala, and their biovolume in the settling particles varies between 0% and 92% (on average 30 ± 28 (SD) %, n = 53) of total monthly biovolume (Fig. 2E). The green microalga *Tetraedron minimum* is usually the dominant species, constituting up to almost 100% of total Chlorophyte biomass (on average 67 ± 30%, n = 53). The time series of Chlorophyte biovolume flux at 35 m is comparable with that in the SPM during the overlapping interval (Fig. 2F); both are characterized by a large peak in abundance from July to November 2014. However, in contrast with the diatoms (Fig. 2C), a small shift in the timing of peak maxima can be observed, with Chlorophytes biovolume peaking slightly earlier in the SPM. This may be due to the different sinking rates of diatoms and Chlorophytes: diatoms contain a silica frustule, while the cell wall of *T. minimum* is composed of an aliphatic biopolymer (e.g., Blokker et al., 1998, 2000), which promotes buoyancy and, thus, to a slower descent through the water column.

Previous studies have indicated that C_{23}, C_{25} and C_{27} *n*-alk-1-enes (Castañeda et al., 2009; van Bree et al., 2014) and C_{21} and C_{23} *n*-alkanes are biomarkers for Chlorophytes, and *T. minimum*, in particular (van Bree et al., 2018b). In support of this aquatic origin, the flux-weighted average $\delta^{13}C$ of C_{25} and C_{27} *n*-alk-1-enes in the settling particles (−37.1‰ and −37.4‰, respectively) and of the even more ^{13}C-depleted C_{21} and C_{23} *n*-alkanes (−40.1‰ and −38.7‰, respectively) are comparable to the $\delta^{13}C$ signatures of these biomarkers in SPM (van Bree et al., 2018b). These authors interpreted the strong ^{13}C depletion as evidence for occurrence in Lake Chala of chemically enhanced diffusion and fractionation processes. Chemically enhanced diffusion is characterized by strong stable carbon-isotopic fractionation (Mook et al., 1974) when surface-water pH is high, due to the reaction of CO_2 with OH^- instead of H_2O to form HCO_3^- (Herczeg and Fairbanks, 1987; Bade and Cole, 2006). The pH in Lake Chala is elevated (>9) at times of high primary productivity (van Bree et al., 2018b), which indeed fits with the high abundance in SPM and high flux at 35 m of these ^{13}C-depleted *n*-alk-1-enes and *n*-alkanes. Overall similarity of the $\delta^{13}C$ values of these Chlorophyte biomarkers, in combination with similar temporal trends in flux and abundance of these markers in SPM and those of Chlorophyte biovolume (i.e., all show high abundance from July to November 2014; Fig. 2E-G) strongly support the hypothesis that they are mainly produced by *T. minimum*.

Long-chain fatty acids ($\geq C_{24}$ FAs) are major constituents of the leaf waxes of terrestrial vascular plants, and therefore often used as biomarkers for vascular plants in paleoclimate reconstruction (e.g., Feakins and Eglinton, 2005; Tierney et al., 2008, 2011; Holland et al., 2013). However, van Bree et al. (2018b) showed that also the C_{28} FA in SPM of Lake Chala is predominantly of aquatic origin, possibly produced by Chlorophytes. This was based on its depleted ^{13}C content in SPM (average around −40‰) and seasonal shifts therein of up to 12‰. Although the C_{28} FA has been found in cultures of *T. minimum* and is a building block of its algaenan (Blokker et al., 1998), van Bree et al. (2018b) hesitated to definitely assign the main source of C_{28} FA to *T. minimum* since the occurrence of the C_{28} FA in SPM (Fig. 2H) peaked slightly later than living *T. minimum* biomass (Fig. 2E). Our new data on C_{28} FA in the longer time series of settling particles are in line with *T. minimum* being their predominant origin. Firstly, its $\delta^{13}C$ values vary between −36 and −44‰ (Fig. 3C), in good agreement with SPM data (van Bree et al., 2018b), showing two periods with strong ^{13}C depletion (November 2011 to March 2012, and October 2014 to January 2015), as well as shorter or less intense periods of depletion (e.g., June-July 2011, July and November 2012, June-July 2013, and February 2014; Fig. 3C). In contrast, the C_{26} FA shows much less negative $\delta^{13}C$ values (ca. −26‰) at specific periods of higher flux (i.e., September in 2010 and 2013; Fig. 3A and C), not seen in the flux record of the C_{28} FA (Fig. 3B). These data are consistent with a second source of the C_{26} FA, namely terrestrial vascular plants, during some periods of trap deployment, contrasting with *T. minimum* continually being the predominant source of the C_{28} FA. Secondly, the flux pattern of the C_{28} FA generally fits with the time series of its concentration in SPM (Fig. 2H) and with the flux pattern and SPM abundance of Chlorophyte biovolume (Fig. 2E). These peaks are all broader than those of diatom biovolume (Fig. 2C), revealing that production and settling of *T. minimum* occurs well into the stratification season, up to November in 2014.

Like diatoms, Chlorophyte algae were exceptionally abundant

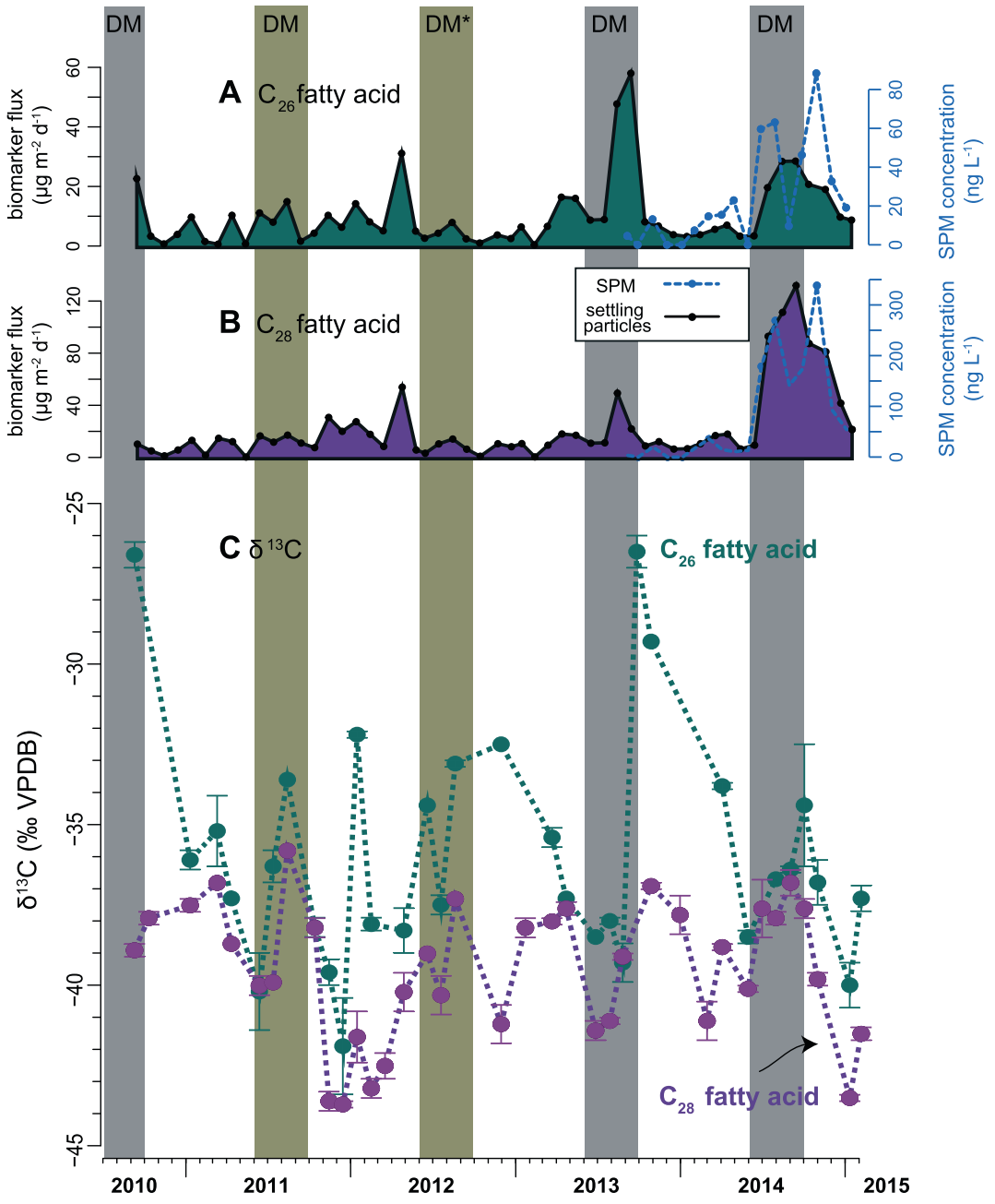


Fig. 3. Settling fluxes and stable carbon-isotopic composition ($\delta^{13}C$) of long-chain fatty acids in Lake Chala between September 2010 and January 2015. For comparison, average fatty acid concentrations in surface-water SPM (0–10–25 m) between September 2013 and January 2015 (van Bree et al., 2018b) are shown. Vertical bands as in Fig. 2. (A) Flux of the C_{26} fatty acid in settling particles (solid black line) and its concentration in surface-water SPM (dashed blue line). (B) Flux of the C_{28} fatty acid in settling particles (solid black line) and its concentration in surface-water SPM (dashed blue line). (C) $\delta^{13}C$ of the C_{26} (dashed green line) and C_{28} (dashed purple line) fatty acids in settling particles. Error bars indicate ± standard deviation of the measurements.

during the 17-month period of SPM sampling with as notable difference that the first bloom phase of the diatoms (September 2013) is not seen in the Chlorophyte records. With regard to the 53-month settling particle record, few similarities can be drawn between the two phytoplankton groups. Interestingly, the peak in Chlorophytes is not recurring annually, and although not absent, only low concentrations of Chlorophyte biomarkers and biovolume were found between September 2010 and June 2014. Therefore, based on the currently available sediment-trap record, it seems not possible to predict if and when a bloom of Chlorophytes will develop in a specific year.

3.1.3. *Eustigmatophyceae biomarkers*

C_{30} and C_{32} 1,15 long-chain diols (LCDs) are known Eustigmatophyceae biomarkers, also in lacustrine environments (e.g., Volkman et al., 1999; Rampen et al., 2014). Villanueva et al. (2014) studied LCDs in SPM from the upper 25 m of the water column collected in February 2010. The C_{30} and C_{32} 1,15- and C_{34} 1,17-diols were most abundant, and the maximum in their summed concentration at 9 m water depth coincided with a maximum in Eustigmatophyceae 18S rRNA gene copies, signifying Eustigmatophyceae algae as important producers of LCDs. 18S rRNA gene clone libraries revealed three known and two novel groups of Eustigmatophyceae families, of which the latter two predominate, which may explain the unusually high (i.e., ca. 10%) fractional abundance of the C_{34} 1,17-diol. In the 17-month SPM study conducted by van Bree et al. (2018b) LCDs turned out to be most abundant during periods of strong water-column stratification in

November 2013, May 2014 and November 2014 (Fig. 4). Again, C_{30} and C_{32} 1,15-diols were the most abundant LCDs.

In this study, LCDs were analyzed in settling-particles collected between August 2011 and January 2015 (i.e., 43 months). In addition to C_{30} and C_{32} 1,15-diols, we also quantified the C_{30} 1,14-, C_{30} 1,13-, and C_{34} 1,17-diols using SIM. Some 1,14-diols are frequently encountered in freshwater systems (Lattaud et al., 2017, 2018), although their sources are unclear. Only *Pseudostaurastrum enorme*, a freshwater Eustigmatophyceae species that occurs in lakes is known to produce C_{28} 1,14- and C_{30} 1,14-diols in culture (Rampen et al., 2014) but the C_{28} 1,14-diol was not detected in the settling particles from Lake Chala. Both the fluxes of LCDs and their distributions varied over time (Fig. 4). The C_{30} and C_{32} 1,15-diols were the most common LCDs (both 30 ± 20%), whereas the C_{30} 1,14- and 1,13-diols were present in lower abundances (10 ± 5% and 3 ± 3%, respectively), and the C_{34} 1,17-diol was only detected during some periods, especially at times of highest total LCD flux (Fig. 4). Fluxes of the different LCDs all followed a similar seasonal pattern. Summed fluxes of LCDs ranged from <1 to 55 μg m^{-2} d^{-1}, peaking in April/May of 2012, 2013, and, to a much lesser extent, 2014 (Fig. 4). Other (sub)maxima are noted in August 2013 and November 2013 and 2014. Due to the often small size, microscopic estimates of the biovolume of Eustigmatophyceae are unfortunately not available to confirm these trends as cell counts were restricted to cells ≥3 μm. The time series of LCD concentration in the SPM and of the LCD flux in settling particles match to some extent (Fig. 4), but not as clear-cut as in the case of diatoms and Chlorophytes. This may have to do with the fact that during the interval of SPM sampling (September 2013–January 2015) LCD production was much reduced compared to 2012 and early 2013. Further, the small size of Eustigmatophyceae likely requires cell senescence to be supplemented with processes such as zooplankton grazing and excretion for efficient downward flux of LCDs.

The LCD flux mainly peaks between February and May 2012 and in April-May 2013 (Fig. 4). The study by Villanueva et al. (2014) of LCD fluxes in Lake Chala from August 2009 to August 2010 showed a similar pattern, namely the summed LCD flux reached a distinct maximum in April 2010. This suggests that ambient conditions during stratified periods in 2010, 2012, and 2013 were more favorable for Eustigmatophyceae proliferation than during the stratification periods between September 2013 and January 2015. Apparently, the remarkably shallow depth of the oxycline (ca. 15 m) during the latter stratified periods provided conditions that allowed other biota to bloom and to compete with the Eustigmatophyceae. During DM periods the LCD flux is typically at a minimum, indicating that elevated nutrient concentrations in the photic zone of the lake benefit diatoms and Chlorophytes more than the Eustigmatophyceae. This is in good agreement with a study of Lake Geneva, where LCDs were most abundant in surface water from late spring to early autumn, coinciding with the relative nutrient depletion during thermal stratification of the water column (Lattaud et al., 2021).

3.1.4. *Cyanobacterial biomarkers*

Our cyanobacterial biovolume estimates in the settling particle flux are limited to the size fraction ≥3 μm. This does not significantly influence the filamentous taxa (including *Planktolyngbya* and related taxa) but could influence estimates of total cyanobacterial biovolume by unknown contribution of small free living coccoid cyanobacteria. However, microscopic identification and counting of living phytoplankton in unfiltered water samples covering 17 months (van Bree et al. 2018b) indicated that such small species do not represent a large proportion of cyanobacteria in Lake Chala. The total cyanobacterial biovolume in settling particles shows two distinct maxima in September 2011 and January 2012 (Fig. 5C), whereas that of *Planktolyngbya* peaks in August 2013 (Fig. 5B). However, *Planktolyngbya* spp. consistently comprise only a minor fraction of the total cyanobacterial biovolume. More notably, peaks of total cyanobacterial biovolume in the SPM record are not reflected in the settling-particle record (Fig. 5C). This is probably caused by the fact that overall cyanobacterial production was very low during the period of SPM monitoring compared to before September 2013 as judged from the settling-particle time series (Fig. 5C).

The C_{19} *n*-alkene was identified as a possible biomarker for cyanobacteria (more specifically, *Planktolyngbya* and related taxa) in Lake Chala (van Bree et al., 2018b), mainly based on its joint peak abundance in SPM and living phytoplankton during SM episodes in January-

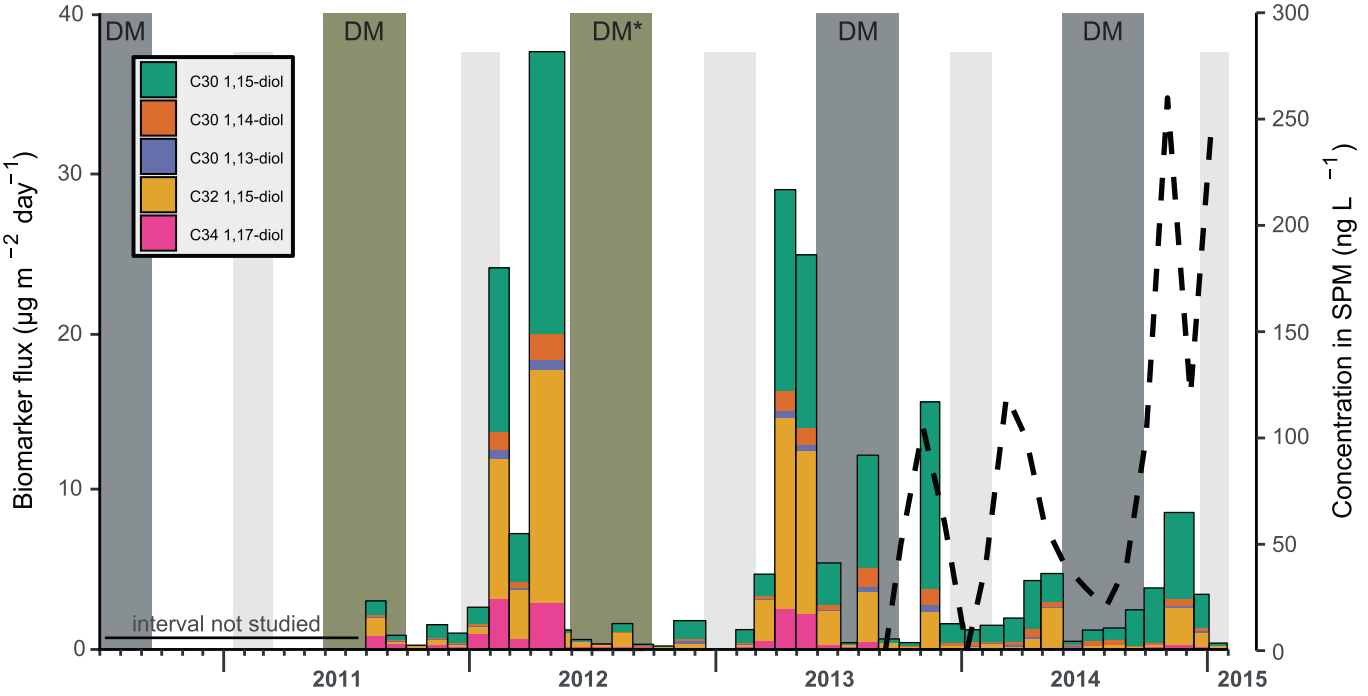


Fig. 4. Summed settling flux and distribution of C_{30}–C_{34} LCDs in Lake Chala between August 2011 and January 2015, determined from settling particles at 35 m water depth. For comparison, average summed C_{30} and C_{32} 1,15-diol concentration in surface-water SPM (0–10–25 m) between September 2013 and January 2015 (van Bree et al., 2018b) are shown. Vertical bands as in Fig. 2.

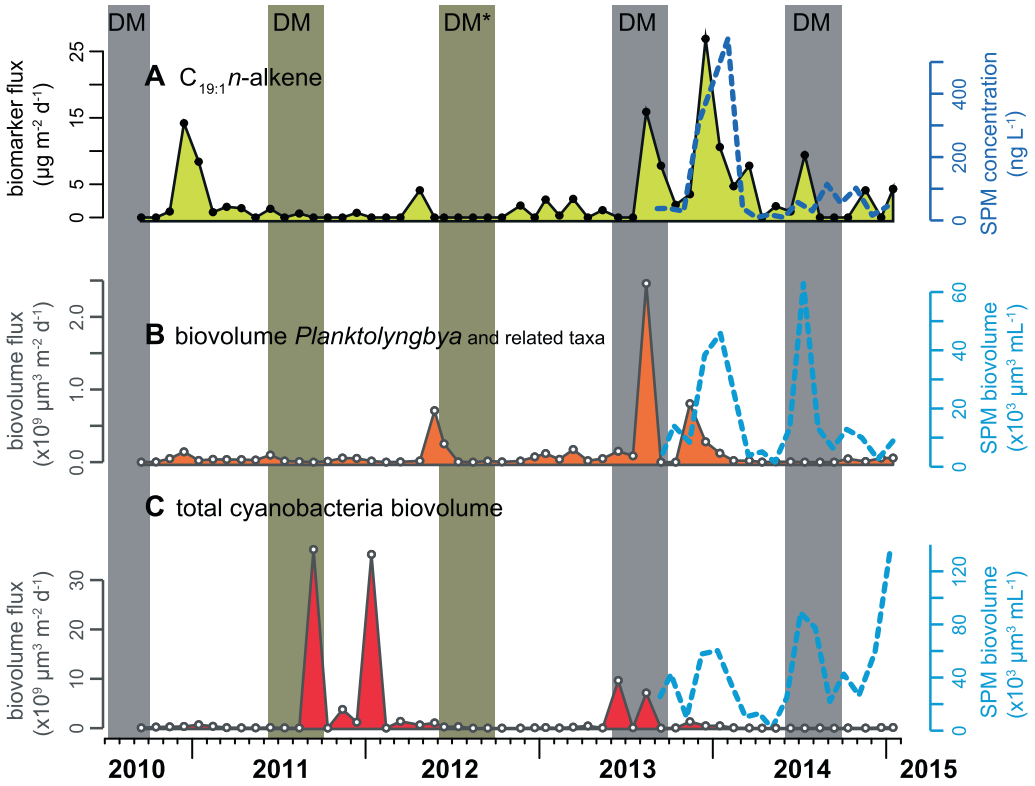


Fig. 5. Biovolume fluxes of total and specific cyanobacteria and of a presumed cyanobacterial biomarker in Lake Chala between September 2010 and January 2015, determined from settling particles at 35 m water depth. For comparison, average cyanobacterial biovolume (0–10–20 m) and average biomarker concentration in surface-water SPM (0–10–25 m) between September 2013 and January 2015 (van Bree et al., 2018b) are shown. (A) Flux of the presumed cyanobacterial biomarker $C_{19:1}$ *n*-alkene (solid black line) and its concentration in SPM (dashed blue line). (B) Biovolume flux of *Planktolyngbya* and related taxa (solid gray line) and their biovolume in surface water (dashed light blue line). (C) Total biovolume flux of cyanobacteria (solid gray line) and total cyanobacteria biovolume in surface water (dashed light blue line). Vertical bands as in Fig. 2.

February (Figs. 5A–B). This specific alkene has indeed been identified in a culture of a *Planktolyngbya* sp. (Zhu et al., 2018). In our longer time series of settling particles, there are two periods with increased $C_{19:1}$ *n*-alkene flux: from December 2010 to January 2011, and from August 2013 to March 2014, with the highest recorded flux (27 µg m^{-2} d^{-1}) being reached in December 2013 (Fig. 5A). The timing of seasonal variation in $C_{19:1}$ *n*-alkene flux differs from that of all other biomarkers in the settling particles, but is, to some extent, comparable to that of $C_{19:1}$ *n*-alkene concentrations in SPM during the overlapping period (van Bree et al., 2018b; Fig. 3A). The main difference between the settling-particle and SPM time series are the increased $C_{19:1}$ *n*-alkene fluxes during the transition from DM to stratified conditions in September 2013; and its high flux in July 2014, neither of which is reflected in the SPM (Fig. 3A). The flux of the $C_{19:1}$ *n*-alkene is only poorly correlated with *Planktolyngbya* biovolume ($R^2 = 0.16$, $p < 0.01$, $n = 53$), and does not correlate at all with total cyanobacterial biovolume ($R^2 = 0.005$, $p = 0.63$, $n = 53$). This can be readily explained by the fact that *Planktolyngbya* only represents a small fraction of all cyanobacteria in the particle flux and that the C_{19} *n*-alkene can also be produced by other cyanobacteria (Coates et al., 2014; Zhu et al., 2018). Thus, based on our current understanding, the $C_{19:1}$ *n*-alkene record in settling particles represents cyanobacteria that bloom when SM provides the surface waters with a modest concentration of nutrients under ambient conditions otherwise unfavorable for diatom blooms.

3.2. Other biomarkers

3.2.1. Bacterial biomarkers

The *ai*-C_{15}, *i*-C_{15}, *i*-C_{16} and *i*-C_{17} FAs are generally considered as non-specific bacterial biomarkers (e.g., Kaneda, 1991; Boschker and Middelburg, 2002). This is reflected in the record of their summed flux over time showing less distinct maxima and minima (Fig. 6A) than observed for phytoplankton-derived biomarkers. The temporal variation of these bacterial biomarkers in settling particles is to some extent comparable to that in SPM (Fig. 6A), with the highest values in August-September 2013 (ca. 240 µg m^{-2} d^{-1}). The settling flux of bacterial biomarkers mainly increases during periods of SM (January to May 2012, February to April 2014) or DM (July to September 2011, April to October 2013, July to December 2014). Higher fluxes of bacterial biomarkers during and after phytoplankton blooms is to be expected, as those blooms contribute to the pool of decaying organic matter that heterotrophic bacteria remineralize. Nevertheless, succession of phytoplankton blooms by peak fluxes of bacterial biomarkers is not clear-cut, as not all phytoplankton blooms coincide with or are followed by high bacterial biomarker fluxes. For example, peak fluxes of the bacterial FAs occur in August 2014, coinciding with high levels of Chlorophytes, but high fluxes in September 2010 do not correspond with increases in any biomarker, and the peak flux of bacterial FAs in August 2013 (Fig. 6A) precedes the peak diatom flux (Fig. 2C).

3.2.2. Isoarborinol

Isoarborinol and its degradation products are typically found in crater lakes and tropical lacustrine settings with permanently anoxic bottom waters and sediments (e.g., Jaffé and Hausmann, 1995; Hanisch et al., 2003; van Bree et al., 2018a). A suite of isoarborinol degradation products was found in the sediments of Lake Chala, where their concentrations were higher during inferred wetter periods in the past, and under stratified conditions in the modern lake (van Bree et al., 2018a). The concentration of isoarborinol in the 4.5-year record of settling particles studied here was generally below detection limit, except during

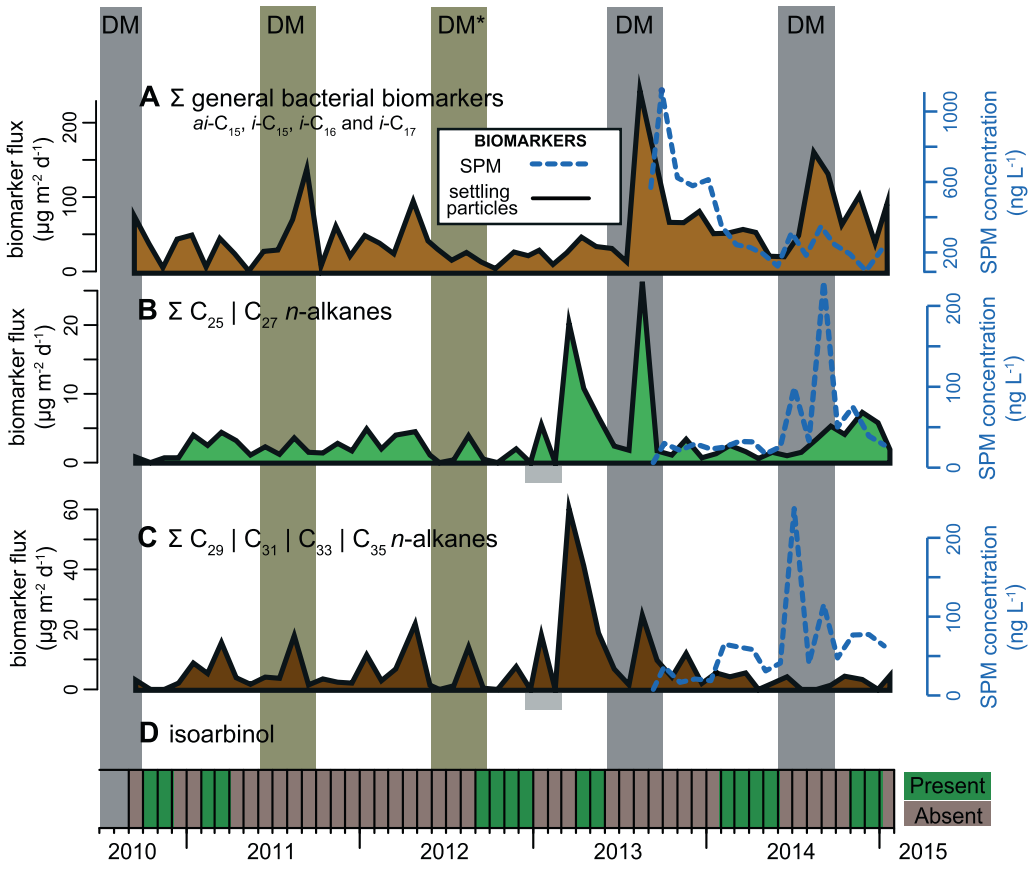


Fig. 6. Settling fluxes of general bacterial biomarkers and *n*-alkanes in Lake Chala between September 2010 and January 2015, determined from settling particles at 35 m depth. For comparison, their average concentrations in surface-water SPM (0–10-25 m) between September 2013 and January 2015 (van Bree et al., 2018b) are shown. (A) Summed flux of *ai*-C_{15}, *i*-C_{15}, *i*-C_{16} and *i*-C_{17} fatty acids in settling particles (solid black line) and their summed concentration in surface-water SPM (dashed blue line). (B) Summed flux of C_{25} and C_{27} *n*-alkanes in settling particles (solid black line) and their summed concentration in surface-water SPM (dashed blue line). (C) Summed flux of C_{29}, C_{31}, C_{33} and C_{35} *n*-alkanes in settling particles (solid black line) and their summed concentration in surface-water SPM (dashed blue line). (D) Traces (presence) of isoarborinol in settling-particle samples (green bars). Vertical bands as in Fig. 2.

periods with a stratified water column, i.e. in October-November 2010, February-March 2012, September to December 2012; March-April 2013; February to May 2014 and November-December 2014, when isoarborinol was detected in small amounts. Because of the persistently low concentrations and co-elution with other compounds, isoarborinol was not quantified, but its presence/absence is indicated in Fig. 6D. The specific aerobic microbial source organism of isoarborinol is unknown (see van Bree et al., 2018a), but the occurrence of isoarborinol indicates that its source organism prefers stratified water-column conditions, thus supporting the use of isoarborinol and its degradation products as a proxy for strong stratification.

3.2.3. *Vascular plant leaf wax lipids*

C_{29} to C_{35} long-chain *n*-alkanes are well-established leaf-wax biomarkers (Eglinton and Hamilton, 1967). Sinninghe Damsté et al. (2011) used *n*-alkanes with chain lengths ≥31 extracted from a 25,000-year (25-kyr) sediment record of Lake Chala as markers for vascular plant waxes based on the distributions and $\delta^{13}C$ values of *n*-alkane homologues. This revealed a marked transition in local lowland vegetation from being dominated (~70–100%) by C_4 plants during the glacial period until 16.5 cal kyr BP, to a more mixed C_3/C_4 plant composition (~30–60% C_4) during the Holocene. In our settling-particle record, fluxes of the C_{29} to C_{35} *n*-alkanes show similar temporal variation (R^2 values varying 0.55–0.85, $p < 0.001$, $n = 53$), indicating a shared origin. This implies that all *n*-alkanes ranging from C_{29} to C_{35} can here be considered as terrestrial plant wax biomarkers. As expected, temporal variation in these long-chain *n*-alkanes (Fig. 6C) is clearly different than that of the Chlorophyte-derived C_{21} and C_{23} *n*-alkanes (Fig. 2G), but more similar to that of the C_{25} and C_{27} *n*-alkanes (Fig. 6B), which in Lake Chala are considered a mix of terrestrial and aquatic *n*-alkanes (Sinninghe Damsté et al., 2011; van Bree et al., 2018b). Van Bree et al. (2018b) reported that vascular plant wax biomarkers are present in SPM in variable but generally low concentration (Fig. 6C), while they are clearly present in the sediments of Lake Chala (Sinninghe Damsté et al., 2011). This mismatch was explained by the 'snapshot' nature of SPM, which mainly represents biomarkers that are present in the water column at the time of sampling, and not necessarily reflects those that are transferred to the sediments. Indeed, C_{29} to C_{35} *n*-alkanes were present in settling particles throughout the sampling period (Fig. 6B), although their summed flux (typically below 10 µg m^{-2} d^{-1}) is an order of magnitude lower than the summed flux of aquatic (diatom and Chlorophyte) biomarkers. A markedly higher flux of summed plant wax *n*-alkanes than during the period of SPM monitoring occurred in March-April 2013, reaching 60 µg m^{-2} d^{-1}. Also during 2011–2012 it regularly exceeded 10 µg m^{-2} d^{-1} (Fig. 6C). Hence, it seems that low (trace) amounts of C_{29} to C_{35} long-chain *n*-alkanes in settling particles during the SPM sampling period truly reflect very low input to the lake, perhaps related to lower-than-average windiness reducing their mobilization from vegetation and leaf litter surrounding the lake.

Several proxies based on the distribution of *n*-alkanes are used to reconstruct aspects of paleovegetation. The carbon preference index (CPI) is used as a measure of *n*-alkane origin, where high CPI values are indicative of a plant wax origin and represent the strong odd-over-even *n*-alkane distribution of vascular plants, while bacterial or algal sources

have CPI values ~1 (Gelpi et al., 1970; Cranwell et al., 1987). CPI values in monthly settling-particle samples from Lake Chala range between 0.4 and 14 (3.3 ± 2.8, $n = 43$), indicating the presence of both aquatic and terrestrial sourced *n*-alkanes. Furthermore, the average chain length (ACL) is often used as an indicator of vegetation type (Freeman and Pancost, 2014; Garcin et al., 2014; Diefendorf and Freimuth, 2017). In Africa, higher ACL values reflect greater abundance of C_4 grasses (C_{31} dominated, relatively high contribution of C_{33}) and C_3 savannah vegetation (C_{31} dominated) compared to rainforest trees and shrubs that are thought to produce more C_{27} and C_{29} *n*-alkanes (e.g., Rommerskirchen et al., 2006; Vogts et al., 2009, 2012; Bush and McInerney, 2013). In Lake Chala settling particles, monthly ACL values range from 23.0 to 29.6 (27.2 ± 2.0, $n = 51$). As ACL also includes the aquatic C_{23} to C_{27} *n*-alkanes, it is not possible to reconstruct the (paleo)vegetation type using this proxy. Instead, ACL values in Lake Chala are indicative of a predominantly aquatic vs a leaf wax origin of *n*-alkanes. Given the multitude of factors influencing the relative proportion of these two groups (e.g., changes in lake level, physical and chemical water column properties, vegetation cover) the ACL proxy in Lake Chala offers little meaningful information on the vegetation type sourcing the *n*-alkanes.

3.3. Seasonal and multi-annual trends in settling biomarker fluxes: implications for the sediment record

Our analysis of the 53-month time series of settling-particle fluxes, discussed alongside the findings from detailed SPM data covering 17 months, reveals a fuller picture of seasonal to multi-annual trends in the occurrence and distribution of organic biomarkers in Lake Chala. Considerable variation is observed throughout the year, mainly governed by seasonal changes in physical properties of the lake, i.e., the mixing and stratification of the water column. For instance, proliferation of diatoms and Chlorophytes is driven by nutrients that are brought into the photic zone during DM (Figs. 2, 7A–C). The low-nutrient conditions during stratification subsequently create opportunities for other autotrophs. For example, Eustigmatophyceae profit from the more stagnant conditions during and at the end of stratification (Figs. 4, 7G). Also, cyanobacteria can outcompete other phytoplankton under low nutrient conditions, as is reflected by the high concentrations of $C_{19:1}$ *n*-alkene during shallow mixing during strong stratification periods (Figs. 5A, 7D). Furthermore, mixing and stratification also influences the heterotrophic bacterial community of Lake Chala. Bacterial biomarkers tend to be more prevalent during periods of strong stratification (Figs. 6, 7H), presumably because they thrive when oxygen-depleted conditions extend upward in the hypolimnion. The high flux of biomarkers from anoxic archaea (that are mainly prevalent in the deepest water column) in the settling particles from September 2013 to August 2014, as revealed by high isoGDGT-0 / crenarchaeol ratios (Fig. 7F; Baxter et al., 2021), indicates that the oxycline was exceptionally shallow during this time.

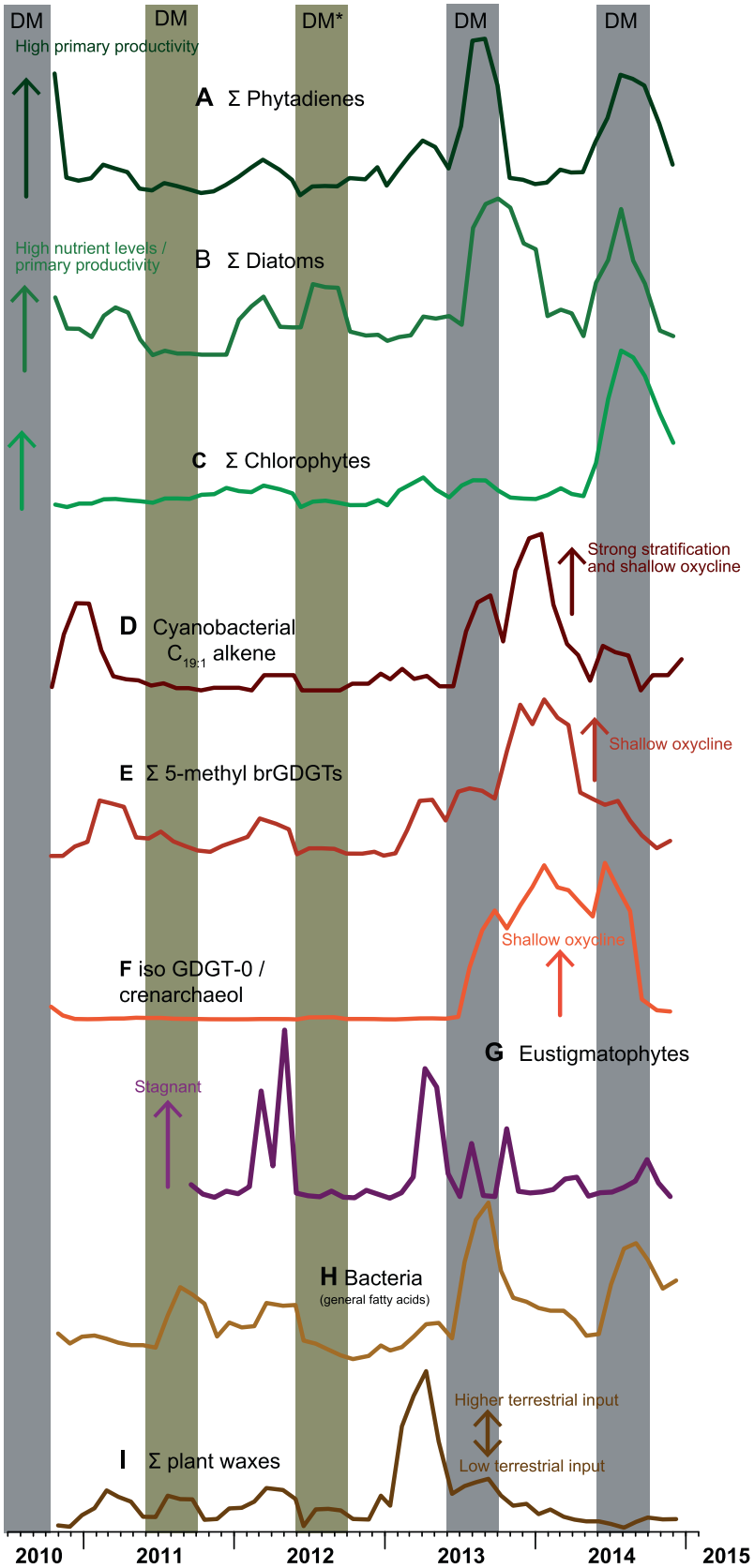
At first glance, the period of extensive SPM and water-column monitoring between September 2013 and January 2015 seems to have presented microbial communities of Lake Chala with habitat conditions deviating from those during the other years covered by the settling-particle time series (Fig. 7). Indeed the flux of phytoplankton cells and biomarkers is much lower during the three years preceding this period (Figs. 7A–D). Moreover, there is very little terrestrial input during the SPM period (Fig. 7I). Water-column monitoring data show that the oxycline was very shallow during stratification in 2013–2014 (van Bree et al., 2018b), which is reflected in high isoGDGT-0/crenarchaeol values (Fig. 7F), driven by the reduced niche for crenarchaeol-producing Nitrosphaerota under these conditions (Baxter et al., 2021). Although the period from September 2013 to January 2015 seems to stand out in this time series (Baxter et al., 2021), the occurrence of a period with similarly high isoGDGT-0/crenarchaeol values between July 2008 and November 2009 (Sinninghe Damsté et al., 2009; Buckles et al., 2014, 2016) suggests that certain water-column conditions and their associated biomarker distributions recur on multi-annual rather than seasonal timescales. Hence, the order of appearance and temporal trends in terrestrial and aquatic biomarkers observed in this study do not necessarily indicate that any microbial succession is annually recurring or predictable.

The observed low-frequency variation in biomarker-inferred microbial community composition suggests an important role for threshold effects in this lake system. This is illustrated by the binary behavior of certain biomarkers. For example, Chlorophytes are a major constituent of the primary producers, or they are not (Figs. 2A and E; van Bree et al., 2018b). The diatom bloom is dominated by either *Afrocymbella* or *Nitzschia* (van Bree et al., 2018b). Previous research also determined that blooms of Nitrosphaerota develop under stratified conditions with a relatively deep oxycline, or they do not occur at all (Baxter et al., 2021). Branched GDGTs generally thrive in the expanded anoxic waters during stratification, but are dominated by either 5-methyl brGDGT-Ib and IIb or 6-methyl brGDGT-IIa′ (van Bree et al., 2020). This threshold behavior of the microbial community in Lake Chala appears quite drastic considering that inter-annual variation in temperature, rainfall and wind during the 4.5-yr period of sediment-trap sampling are relatively modest. Thus, small physical and/or chemical disturbances of the water column can obviously trigger large changes in the microbial community. It has been proposed that changes in the metabolism of temperate, oligotrophic lakes seem to be subtle and sensitive to short-term changes in physical parameters, such as precipitation, wind and thermal stratification (e.g., Richardson et al., 2017). Indeed, our biomarker records from tropical Lake Chala confirm this large and dynamic variability in primary productivity, as well as bacterial and archaeal activity with depth (van Bree et al., 2018b, 2020; Baxter et al., 2021) and over time. Admittedly, the threshold behavior observed in certain biomarkers and their associated proxies, could, to some degree, also be an artefact of the position of the sediment trap at 35 m water depth. Considering that the spatial distribution of many biomarkers is strongly controlled by the depth of the oxycline, small differences in the height of the oxycline in relation to sediment trap depth could have resulted in drastic differences in the organic material capture in the sediment trap, but more subtle differences if considering the full water column.

Nonetheless, the observed threshold behavior of microbial populations in modern-day Lake Chala indicates that subtle environmental variability can have a large impact on aquatic microbial communities, and thus on the relative abundance of taxon-specific biomarker stored in the sediment record. This sensitivity to subtle changes is a treasure trove for proxy applications and paleoclimate reconstruction, as it allows to reconstruct past environmental parameters, including monsoon intensity, temperature, primary productivity / nutrient availability. It is clear, however, that 53 months of sediment trap data, or 17 months of SPM depth profiles, is not nearly long enough to capture the full range of inter-annual variability of the lake's microbial community, and to identify the (climatic) drivers of threshold systems such as Lake Chala. This supports the earlier suggestions (Buckles et al., 2016; van Bree et al., 2020; Baxter et al., 2021) that to fully unravel the dynamics of lake systems, monitoring programs need to extend over substantially longer time scales than are usually considered.

4. Conclusion

Large seasonal and inter-annual variation in aquatic biomarker fluxes in Lake Chala are observed for a large variety of microbiota such as diatoms, Chlorophytes, Eustigmatophyceae, and bacteria. Based on the sediment-trap data obtained, the occurrence of certain biomarkers can be linked to seasonally recurring periods of mixing and stratification of the water column, however, also major variation is evident between consecutive years. Notably, seemingly similar open-water conditions can trigger different microbial communities to flourish. At this stage it is not certain what drives this threshold behavior and how this impacts the microbial community over longer time periods. This demonstates that



(caption on next page)

Fig. 7. Time series of biomarker fluxes in Lake Chala between August 2010 and January 2015, presented as three-month running averages to highlight periods of high primary productivity (A-C), stratification and shallow oxycline (D-F), stagnant water conditions (G), bacterial activity (H-I) and vegetation (J). Each time series is normalized to the highest flux measured for the given biomarker, based on absolute monthly fluxes as plotted in Figs. 2–6. Temporal variation in primary productivity is represented by (A) summed phytadiene flux for total productivity, (B) summed (iso)loliolide flux for diatom productivity, and (C) summed fluxes of $C_{23:1}$, $C_{25:1}$ and $C_{27:1}$ *n*-alk-1-enes, C_{21} and C_{23} *n*-alkanes, and the C_{28} fatty acid for Chlorophyte algae. Periods of strong stratification and shallow oxycline are indicated by (D) flux of the cyanobacterial $C_{19:1}$ *n*-alkene, (E) summed flux of 5-methyl brGDGTs (van Bree et al., 2020), and (F) the isoGDGT-0/crenarchaeol ratio (Baxter et al., 2021). Stagnant water conditions are indicated by (G) the summed flux of C_{30} and C_{32} 1,15 diols derived from Eustigmatophyte algae. Bacterial biomass is represented by (H) the summed flux of *ai*-C_{15}, *i*-C_{15}, *i*-C_{16}, *i*-C_{17}, C_{20} and C_{22} fatty acids. The input of terrestrial material is represented by (I) the summed flux of C_{29}–C_{35} *n*-alkanes. Vertical bands as in Fig. 2.

biomarker monitoring of modern lake systems need to be carried out over substantially longer time scales than usually applied to fully unravel and understand their biomarker dynamics. Furthermore, chemically enhanced fractionation was shown to be a regular feature in the water column of Lake Chala. This process thus exerts an important influence on the sedimentary $\delta^{13}C$ signature of aquatic biomarkers and, consequently, also that of bulk organic matter stored in the sediments, which is assumed to derive predominantly from algal material.

Data availibility

Data are available through Mendeley Data at doi: https://doi.org/10.17632/tgsxb83wgf.1.

CRediT authorship contribution statement

J.S. Sinninghe Damsté: Writing – review & editing, Writing – original draft, Visualization, Supervision, Project administration, Investigation, Conceptualization. **L.G.J. van Bree:** Writing – original draft, Visualization, Formal analysis, Conceptualization. **J. Lattaud:** Writing – review & editing, Formal analysis, Investigation. **P. de Regt:** Formal analysis. **C. Cocquyt:** Writing – review & editing, Formal analysis. **A.J. Baxter:** Writing – original draft. **J.W. de Leeuw:** Writing – review & editing, Supervision, Conceptualization. **D. Verschuren:** Writing – review & editing, Writing – original draft, Supervision, Resources, Project administration, Funding acquisition, Data curation, Conceptualization. **F. Peterse:** Writing – review & editing, Supervision, Project administration, Conceptualization.

Declaration of competing interest

The authors declare that they have no known competing financial interests or personal relationships that could have appeared to influence the work reported in this paper.

Acknowledgements

We thank C.M. Oluseno for conducting consistent monthly sampling and field assistance in Kenya during the full duration of this study. Sample collection was carried out with permission of the Permanent Secretary of the Ministry of Education, Science and Technology of Kenya, research permit 13/001/11C to D.V. We thank A. Negash for help with lipid extractions. We are grateful to A. van Dijk, D. Kasjaniuk, A. van Leeuwen-Tolboom and K. Nierop at Utrecht University for technical and analytical support, and L. Villanueva for discussion. We also thank three anonymous referees for helpful comments on an earlier draft of this paper. This research was supported by an NESSC Gravitation Grant (024.002.001) from the Dutch Ministry of Education, Culture and Science (OCW) to J.S.S.D. Phytoplankton analyses were done in the frame of the Brain-be project BR/121/A2 PAMEXEA (Patterns and mechanisms of climate extremes in East Africa) financed by Belgium Science Policy (BELSPO).

References

Bade, D.L., Cole, J.J., 2006. Impact of chemically enhanced diffusion on dissolved inorganic carbon stable isotopes in a fertilized lake. J. Geophys. Res. 111, C01014.
Barker, P.A., Hurrell, E.R., Leng, M.J., Wolff, C., Cocquyt, C., Sloane, H.J., Verschuren, D., 2011. Seasonality in equatorial climate over the past 25 k.y. revealed by oxygen isotope records from Mount Kilimanjaro. Geology 39, 1111–1114.
Baxter, A.J., van Bree, L.G., Peterse, F., Hopmans, E.C., Villanueva, L., Verschuren, D., Sinninghe Damsté, J.S., 2021. Seasonal and multi-annual variation in the abundance of isoprenoid GDGT membrane lipids and their producers in the water column of a meromictic equatorial crater lake (Lake Chala, East Africa). Quat. Sci. Rev. 273, 107263.
Baxter, A.J., Verschuren, D., Peterse, F., Miralles, D.G., Martin-Jones, C.M., Maitituerdi, A., Van der Meeren, T., Van Daele, M., Lane, C.S., Haug, G.H., Olago, D. O., Sinninghe Damsté, J.S., 2023. Reversed Holocene temperature–moisture relationship in the Horn of Africa. Nature 620, 336–343.
Baxter, A.J., Peterse, F., Verschuren, D., Maitituerdi, A., Waldmann, N., Sinninghe Damsté, J.S., 2024. Disentangling influences of climate variability and lake-system evolution on climate proxies derived from isoprenoid and branched glycerol dialkyl glycerol tetraethers (GDGTs): the 250 kyr Lake Chala record. Biogeosciences 21, 2877–2908.
Berke, M.A., Johnson, T.C., Werne, J.P., Grice, K., Schouten, S., Sinninghe Damsté, J.S., 2012. Molecular records of climate variability and vegetation response since the Late Pleistocene in the Lake Victoria basin, East Africa. Quat. Sci. Rev. 55, 59–74.
Blokker, P., Schouten, S., van den Ende, H., de Leeuw, J.W., Hatcher, P.G., Sinninghe Damsté, J.S., 1998. Chemical structure of algaenans from the freshwater algae *Tetraedron minimum*, *Scenedesmus communis* and *Pediastrum boryanum*. Org. Geochem. 29, 1453–1468.
Blokker, P., Schouten, S., de Leeuw, J.W., Sinninghe Damsté, J.S., van den Ende, H., 2000. A comparative study of fossil and extant algaenans using ruthenium tetroxide degradation. Geochim. Cosmochim. Acta 64, 2055–2065.
Bodé, S., De Wispelaere, L., Hemp, A., Verschuren, D., Boeckx, P., 2020. Water-isotope ecohydrology of Mount Kilimanjaro. Ecohydrology 13, e2171.
Boschker, H.T.S., Middelburg, J.J., 2002. Stable isotopes and biomarkers in microbial ecology. FEMS Microbiol. Ecol. 40, 85–95.
Buckles, L.K., Villanueva, L., Weijers, J.W.H., Verschuren, D., Sinninghe Damsté, J.S., 2013. Linking isoprenoidal GDGT membrane lipid distributions with gene abundances of ammonia-oxidizing Thaumarchaeota and uncultured crenarchaeotal groups in the water column of a tropical lake (Lake Challa, East Africa). Environ. Microbiol. 9, 2445–2462.
Buckles, L.K., Weijers, J.W.H., Verschuren, D., Sinninghe Damsté, J.S., 2014. Sources of core and intact branched tetraether membrane lipids in the lacustrine environment: anatomy of Lake Challa and its catchment, equatorial East Africa. Geochim. Cosmochim. Acta 140, 106–126.
Buckles, L.K., Verschuren, D., Weijers, J.W.H., Cocquyt, C., Blaauw, M., Sinninghe Damsté, J.S., 2016. Interannual and (multi-) decadal variability in the sedimentary BIT index of Lake Challa, East Africa, over the past 2200 years: assessment of the precipitation proxy. Clim. Past 12, 1243–1262.
Bush, T.R., McInerney, F., 2013. Leaf wax *n*-alkane distributions in and across modern plants: implications for paleoecology and chemotaxonomy. Geochim. Cosmochim. Acta 117, 161–179.
Castañeda, I.S., Werne, J.P., Johnson, T.C., 2009. Influence of climate change on algal community structure and primary productivity of Lake Malawi (East Africa) from the Last Glacial Maximum to present. Limnol. Oceanogr. 54, 2431–2447.
Castañeda, I.S., Schouten, S., 2011. A review of molecular organic proxies for examining modern and ancient lacustrine environments. Quat. Sci. Rev. 30, 2851–2891.
Coates, R.C., Podell, S., Korobeynikov, A., Lapidus, A., Pevzner, P., Sherman, D.H., Allen, E.E., Gerwick, L., Gerwick, W.H., 2014. Characterization of cyanobacterial hydrocarbon composition and distribution of biosynthetic pathways. PLoS One 9, e85140.
Cocquyt, C., Ryken, E., 2016. *Afrocymbella barkeri* spec. nov. (Bacillariophyta), a common phytoplankton component of Lake Challa, a deep crater lake in East Africa. Eur. J. Phycol. 51, 217–225.
Cocquyt, C., Ryken, E., 2017. Two new needle-shaped *Nitzschia* taxa from a deep East African crater lake. Diatom Res. 32, 465–475.
Cranwell, P.A., Eglinton, G., Robinson, N., 1987. Lipids of aquatic organisms as potential contributors to lacustrine sediments II. Org. Geochem. 11, 513–527.
De Crop, W., Verschuren, D., 2021. Mixing regimes in the equatorial crater lakes of western Uganda. Limnologica 90, 125891.
Diefendorf, A.F., Freimuth, E.J., 2017. Extracting the most from terrestrial plant-derived *n*-alkyl lipids and their carbon isotopes from the sedimentary record: a review. Org. Geochem. 103, 1–21.

Eglinton, G., Hamilton, R.J., 1967. Leaf epicuticular waxes: the waxy outer surfaces of most plants display a wide diversity of fine structure and chemical constituents. Science 156, 1322–1335.
Eglinton, T.I., Eglinton, G., 2008. Molecular proxies for paleoclimatology. Earth Planet. Sci. Lett. 275, 1–16.
Feakins, S.J., Eglinton, T.I., 2005. Biomarker records of late Neogene changes in northeast African vegetation. Geology 33, 977–980.
Freeman, K.H., Pancost R.D., 2014. Biomarkers for terrestrial plants and climate. In: Falkowski, P. and Freeman, K., Treatise on Geochemistry, Elsevier, Amsterdam, 12, 395-416.
Garcin, Y., Schefuß, E., Schwab, V.F., Garreta, V., Gleixner, G., Vincens, A., Todou, G., Séné, O., Onana, J.M., Achoundong, G., Sachse, D., 2014. Reconstructing C_3 and C_4 vegetation cover using *n*-alkane carbon isotope ratios in recent lake sediments from Cameroon, Western Central Africa. Geochim. Cosmochim. Acta 142, 482–500.
Gelpi, E., Schneider, H.J., Mann, J., Oró, J., 1970. Hydrocarbons of geochemical significance in microscopic algae. Phytochemistry 9, 603–612.
Grossi, V., Baas, M., Schogt;, N., Klein Breteler, W.C.M., de Leeuw, J.W., Rontani, J.-F., 1996. Formation of phytadienes in the water column: myth or reality? Org Geochem. 24, 833–839.
Hanisch, S., Ariztegui, D., Püttmann, W., 2003. The biomarker record of Lake Albano, central Italy—implications for Holocene aquatic system response to environmental change. Org. Geochem. 34, 1223–1235.
Hemingway, J.D., Schefuß, E., Dinga, B.J., Pryer, H., Galy, V.V., 2016. Multiple plant-wax compounds record differential sources and ecosystem structure in large river catchments. Geochim. Cosmochim. Acta 184, 20–40.
Hemp, A., 2006. Continuum or zonation? Altitudinal gradients in the forest vegetation of Mt. Kilimanjaro. Plant Ecol. 184, 27–42.
Herczeg, A.L., Fairbanks, R.G., 1987. Anomalous carbon isotope fractionation between atmospheric CO_2 and dissolved inorganic carbon induced by intense photosynthesis. Geochim. Cosmochim. Acta 51, 895–899.
Holland, A.R., Petsch, S.T., Castañeda, I.S., Wilkie, K.M., Burns, S.J., Brigham-Grette, J., 2013. A biomarker record of Lake El'gygytgyn, Far East Russian Arctic: investigating sources of organic matter and carbon cycling during marine isotope stages 1–3. Clim. Past 9, 243–260.
Jaffé, R., Hausmann, K.B., 1995. Origin and early diagenesis of arborinone/isoarborinol in sediments of a highly productive freshwater lake. Org. Geochem. 22, 231–235.
Jeffrey, S.W., Vesk, M., 1997. Introduction to marine phytoplankton and their pigment signatures. In: Phytoplankton Pigments in Oceanography: Guidelines to Modern Methods. UNESCO, Paris, pp. 37–84.
Kaneda, T., 1991. Iso-and anteiso-fatty acids in bacteria: biosynthesis, function, and taxonomic significance. Microbiol. Rev. 55, 288–302.
Klok, J., Baas, M., Cox, H.C., de Leeuw, J.W., Schenck, P.A., 1984. Loliolides and dihydroactinidiolide in a recent marine sediment probably indicate a major transformation pathway of carotenoids. Tetrahedron Lett. 25, 5577–5580.
Lattaud, J., Kim, J.H., De Jonge, C., Zell, C., Sinninghe Damsté, J.S., Schouten, S., 2017. The C32 alkane-1, 15-diol as a tracer for riverine input in coastal seas. Geochim. Cosmochim. Acta 202, 146–158.
Lattaud, J., Kirkels, F., Peterse, F., Freymond, C.V., Eglinton, T.I., Hefter, J., Mollenhauer, G., Balzano, S., Villanueva, L., van der Meer, M.T.J., Hopmans, E.C., Sinninghe Damsté, J.S., Schouten, S., 2018. Long-chain diols in rivers: distribution and potential biological sources. Biogeosciences 15, 4147–4161.
Lattaud, J., Balzano, S., van der Meer, M.T.J., Villanueva, L., Hopmans, E.C., Sinninghe Damsté, J.S., Schouten, S., 2021. Sources and seasonality of long-chain diols in a temperate lake (Lake Geneva). Org. Geochem. 156, 104223.
Longo, W.M., Huang, Y., Yao, Y., Zhao, J., Giblin, A.E., Wang, X., Zech, R., Haberzettl, T., Jardillier, L., Toney, J., Liu, Z., 2018. Widespread occurrence of distinct alkenones from Group I haptophytes in freshwater lakes: implications for paleotemperature and paleoenvironmental reconstructions. Earth Planet. Sci. Lett. 492, 239–250.
Loomis, S.E., Russell, J.M., Heureux, A.M., D'Andrea, W.J., Sinninghe Damsté, J.S., 2014. Seasonal variability of branched glycerol dialkyl glycerol tetraethers (brGDGTs) in a temperate lake system. Geochim. Cosmochim. Acta 144, 173–187.
Meyers, P.A., Leenheer, M.J., Eaoie, B.J., Maule, S.J., 1984. Organic geochemistry of suspended and settling particulate matter in Lake Michigan. Geochim. Cosmochim. Acta 48, 443–452.
Martin-Jones, C., Lane, C.S., Blaauw, M., Mark, D.F., Verschuren, D., Van der Meeren, T., Van Daele, M., Wynton, H., Blegen, N., Kisaka, M., Leng, M.J., 2024. The >250-kyr Lake Chala record: a tephrostratotype correlating archaeological, palaeoenvironmental and volcanic sequences across eastern Africa. Quat. Sci. Rev. 326, 108476.
Moernaut, J., Verschuren, D., Charlet, F., Kristen, I., Fagot, M., De Batist, M., 2010. The seismic-stratigraphic record of lake-level fluctuations in Lake Challa: hydrological stability and change in equatorial East Africa over the last 140 kyr. Earth Planet. Sci. Lett. 290, 214–223.
Mook, W.G., Bommerson, J.C., Staverman, W.H., 1974. Carbon isotope fractionation between dissolved bicarbonate and gaseous carbon dioxide. Earth Planet. Sci. Lett. 22, 169–176.
Nankabirwa, A., De Crop, W., Van der Meeren, T., Cocquyt, C., Plisnier, P.-D., Balirwa, J., Verschuren, D., 2019. Phytoplankton communities in the crater lakes of western Uganda, and their indicator species in relation to lake trophic status. Ecol. Indicators 107, 105563.
Nicholson, S.E., 2000. The nature of rainfall variability over Africa on time scales of decades to millenia. Global Planet. Change 26, 137–158.
Payne, B.R., 1970. Water balance of Lake Chala and its relation to groundwater from tritium and stable isotope data. J. Hydrol. 11, 47–58.
Rampen, S.W., Willmott, V., Kim, J.H., Uliana, E., Mollenhauer, G., Schefuß, E., Sinninghe Damsté, J.S., Schouten, S., 2012. Long chain 1,13- and 1,15-diols as a potential proxy for palaeotemperature reconstruction. Geochim. Cosmochim. Acta 84, 204–216.
Rampen, S.W., Datema, M., Rodrigo-Gámiz, M., Schouten, S., Reichart, G.J., Sinninghe Damsté, J.S., 2014. Sources and proxy potential of long chain alkyl diols in lacustrine environments. Geochim. Cosmochim. Acta 144, 59–71.
Randlett, M.-E., Coolen, M.J.L., Stockhecke, M., Pickarski, N., Litt, T., Balkema, C., Kwicien, O., Tomonaga, Y., Wehrli, B., Schubert, C.J., 2014. Alkenone distribution in Lake Van sediment over the last 270 ka: influence of temperature and haptophyte species composition. Quat. Sci. Rev. 104, 53–62.
Repeta, D.J., 1989. Carotenoid diagenesis in recent marine sediments: II. Degradation of fucoxanthin to loliolide. Geochim. Cosmochim. Acta 53, 699–707.
Richardson, D.C., Carey, C.C., Bruesewitz, D.A., Weathers, K.C., 2017. Intra- and inter-annual variability in metabolism in an oligotrophic lake. Aquat. Sci. 79, 319–333.
Rommerskirchen, F., Plader, A., Eglinton, G., Chikaraishi, Y., Rullkötter, J., 2006. Chemotaxonomic significance of distribution and stable carbon isotopic composition of long-chain alkanes and alkan-1-ols in C4 grass waxes. Org. Geochem. 37, 1303–1332.
Russell, M., Rosell-Melé, A., 2005. Preliminary study of fluxes of major lipid biomarker classes in the water column and sediments of Lake Baikal, Russia. Global Planet. Change 46, 45–56.
Sinninghe Damsté, J.S., Ossebaar, J., Abbas, B., Schouten, S., Verschuren, D., 2009. Fluxes and distribution of tetraether lipids in an equatorial African lake: constraints on the application of the TEX_{86} palaeothermometer and BIT index in lacustrine settings. Geochim. Cosmochim. Acta 73, 4232–4249.
Sinninghe Damsté, J.S., Verschuren, D., Ossebaar, J., Blokker, J., van Houten, R., van der Meer, M.T.J., Plessen, B., Schouten, S., 2011. A 25,000-year record of climate-induced changes in lowland vegetation of eastern equatorial Africa revealed by the stable carbon-isotopic composition of fossil plant leaf waxes. Earth Planet. Sci. Lett. 302, 236–246.
Sinninghe Damsté, J.S., Weber, Y., Zopfi, J., Lehmann, M.F., Niemann, H., 2022. Distributions and sources of isoprenoidal GDGTs in Lake Lugano and other central European (peri-) alpine lakes: lessons for their use as paleotemperature proxies. Quat. Sci. Rev. 277, 107352.
Tierney, J.E., Russell, J.M., Huang, Y., Sinninghe Damsté, J.S., Hopmans, E.C., Cohen, A. S., 2008. Northern hemisphere controls on tropical southeast African climate during the past 60,000 years. Science 322, 252–255.
Tierney, J.E., Russell, J.M., Sinninghe Damsté, J.S., Huang, Y., Verschuren, D., 2011. Late quaternary behavior of the East African monsoon and the importance of the Congo Air Boundary. Quat. Sci. Rev. 30, 798–807.
Utermöhl, H., 1931. Neue Wege in der quantitativen Erfassung des Planktons. Verh. Int. Ver. Theor. Angew. Limnol. 5, 567–596.
Utermöhl, H., 1958. Zur Vervollkommnung der quantitativen phytoplankton methodik. Mitt. Int. Ver. Theor. Angew. Limnol. 9, 1–38.
van Bree, L.G.J., Rijpstra, W.I.C., Cocquyt, C., Al-Dhabi, N.A., Verschuren, D., Sinninghe Damsté, J.S., de Leeuw, J.W., 2014. Origin and palaeo-environmental significance of C_{25} and C_{27} *n*-alk-1-enes in a 25,000-year lake-sedimentary record from equatorial East Africa. Geochim. Cosmochim. Acta 145, 89–102.
van Bree, L.G.J., Rijpstra, W.I.C., Al-Dhabi, N.A., Verschuren, D., Sinninghe Damsté, J.S., de Leeuw, J.W., 2016. *Des*-A-lupane in an East African lake sedimentary record as a new proxy for the stable carbon isotopic composition of C_3 plants. Org. Geochem. 101, 132–139.
van Bree, L.G.J., Islam, M.M., Rijpstra, W.I.C., Verschuren, D., van Duin, A.C.T., Sinninghe Damsté, J.S., de Leeuw, J.W., 2018a. Origin, formation and environmental significance of des-A-arborenes in the sediments of an East African crater lake. Org Geochem. 125, 95–108.
van Bree, L.G.J., Peterse, F., van der Meer, M.T.J., Middelburg, J.J., Negash, A.M.D., De Crop, W., Cocquyt, C., Wieringa, J.J., Verschuren, D., Sinninghe Damsté, J.S., 2018b. Seasonal variability in the abundance and stable carbon-isotopic composition of lipid biomarkers in suspended particulate matter from a stratified equatorial lake (Lake Chala, Kenya/Tanzania): Implications for the sedimentary record. Quat. Sci. Rev. 192, 208–224.
van Bree, L.G., Peterse, F., Baxter, A.J., De Crop, W., van Grinsven, S., Villanueva, L., Verschuren, D., Sinninghe Damsté, J.S., 2020. Seasonal variability and sources of in situ brGDGT production in a permanently stratified African crater lake. Biogeosciences 17, 1–36.
Verschuren, D., Sinninge Damsté, J.S., Moernaut, J., Kristen, I., Blaauw, M., Fagot, M., Haug, G.H., CHALLACEA project members, 2009. Half-processional dynamics of monsoon rainfall near the East African Equator. Nature 462, 637–641.
Versteegh, G.J.M., Bosch, H.J., de Leeuw, J.W., 1997. Potential palaeoenvironmental information of C_{24} to C_{36} mid-chain diols, keto-ols and mid-chain hydroxy fatty acids; a critical review. Org. Geochem. 27, 1–13.
Villanueva, L., Besseling, M., Rodrigo-Gámiz, M., Rampen, S., Verschuren, D., Sinninghe Damsté, J.S., 2014. Potential biological sources of long chain alkyl diols in a lacustrine system. Org. Geochem. 68, 27–30.
Vogts, A., Moossen, H., Rommerskirchen, F., Rullkötter, J., 2009. Distribution patterns and stable carbon isotopic composition of alkanes and alkan-1-ols from plant waxes of African rain forest and savanna C3 species. Org. Geochem. 40, 1037–1054.
Vogts, A., Schefuß, E., Badewien, T., Rullkötter, J., 2012. *n*-Alkane parameters from a deep sea sediment transect off southwest Africa reflect continental vegetation and climate conditions. Org. Geochem. 47, 109–119.
Volkman, J.K., Barrett, S.M., Blackburn, S.I., 1999. Eustigmatophyte microalgae are potential sources of C_{29} sterols, C_{22}–C_{28} *n*-alcohols and C_{28}–C_{32} *n*-alkyl diols in freshwater environments. Org. Geochem. 30, 307–318.
Wolff, C., Haug, G.H., Timmermann, A., Sinninghe Damsté, J.S., Brauer, A., Sigman, D. M., Cane, M.A., Verschuren, D., 2011. Reduced interannual rainfall variability in East Africa during the Last Ice Age. Science 333, 743–747.

Wolff, C., Kristen-Jenny, I., Schettler, G., Plessen, B., Meyer, H., Dulski, P., Naumann, R., Brauer, A., Verschuren, D., Haug, G.H., 2014. Modern seasonality in Lake Challa (Kenya/Tanzania) and its sedimentary documentation in recent lake sediments. Limnol. Oceanogr. 59, 1621–1636.

Woltering, M., Werne, J.P., Kish, J.L., Hicks, R., Sinninghe Damsté, J.S., Schouten, S., 2012. Vertical and temporal variability in concentration and distribution of thaumarchaeotal tetraether lipids in Lake Superior and the implications for the application of the TEX_{86} temperature proxy. Geochim. Cosmochim. Acta 87, 136.

Zhu, T., Scalvenzi, T., Sassoon, N., Lu, X., Gugger, M., 2018. Terminal olefin profiles and phylogenetic analyses of olefin synthases of diverse cyanobacterial species. Appl. Environm. Microbiol. 84, e00425–e00518.